IEEE Photonics Journal
An IEEE Photonics Society Publication

Open Access

Collinear Acousto-Optic Filtration With Electronically Adjustable Transmission Function

Volume 11, Number 2, April 2019

Sergey N. Mantsevich
Vladimir I. Balakshy

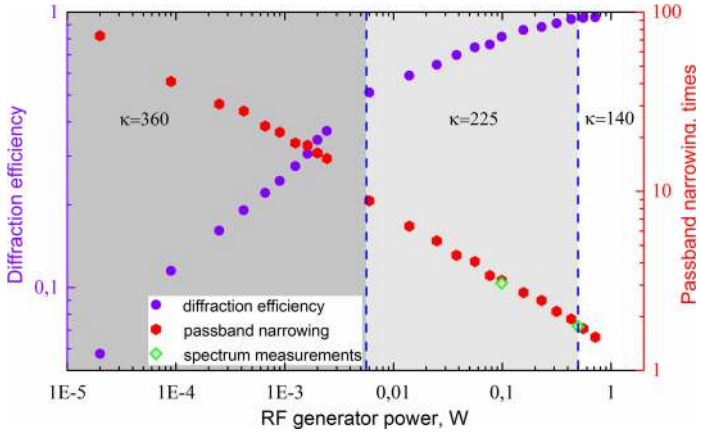

DOI: 10.1109/JPHOT.2019.2899827
1943-0655

IEEE photonics SOCIETY

IEEE

Collinear Acousto-Optic Filtration With Electronically Adjustable Transmission Function

Sergey N. Mantsevich and Vladimir I. Balakshy

Physics Department, M.V. Lomonosov Moscow State University, Moscow 119991, Russia

DOI:10.1109/JPHOT.2019.2899827

Manuscript received December 8, 2018; accepted February 13, 2019. Date of publication February 18, 2019; date of current version March 5, 2019. This work was supported by the Russian Science Foundation (RSF) under Project 18-72-00036. Corresponding author: Sergey N. Mantsevich (e-mail: snmantsevich@yahoo.com).

Abstract: An acousto-optic system containing collinear acousto-optic filter fabricated from calcium molybdate crystal and a positive electronic feedback was examined. The feedback signal is formed due to the optical heterodyning effect that appears for the special geometry of polarizer and analyzer polarization planes mutual orientation between which the collinear filter is located. It is shown that the feedback circuit electrical parameters variation enable controlling the spectral characteristics of the acousto-optic collinear filtration, resulting in enhancing the maximal spectral resolution and transmission function side lobes suppression.

Index Terms: Acousto-optic interaction, collinear acousto-optic filtration, optoelectronic feedback, transmission function, diffraction efficiency.

1. Introduction

To date, acousto-optics occupies an important place in the field of light radiation parameters controlling devices development and manufacturing [1]. It is known that using the acousto-optic (AO) effect, it is possible to control and analyze the optical radiation spectral composition, govern the light beams propagation direction and polarization, and modulate their intensity [2]. AO devices are also used as Q-switchers in optical resonators for the generation of ultra-short laser pulses and are applied in many other optoelectronic devices [3]–[6].

Possessing a number of advantages, such as small dimensions, relatively low power consumption and high reliability, as well as sufficiently high resolving power, the AO devices have also found application in space [7]–[9].

Nevertheless, the optoelectronic devices which operation is based on the acousto-optic effect have some flows. These include the presence of the transmission function side lobes (which is described by the $sinc^2$ function in the ideal case) and the inability of achieving an extremely high spectral resolution. The first drawback means that the AO device has parasitic transmission windows near the main one. The second drawback is related to the fact that the AO device passband is determined by the AO interaction length that is limited by the AO crystal dimensions. But the influence of the light beam divergence [10], complicated acoustic field amplitude and phase structure [11]–[13] and the inhomogeneous temperature distribution inside the crystal increase [14]–[16] with

length of the AO interaction. All the effects mentioned leads to the situation when the spectral resolution either does not increase with a further AO interaction length growth, or even decreases.

The drawbacks mentioned lead to the existence of the areas in optoelectronics, for example, fiber-optic communication, in which AO devices (filters) are rarely used. Modern acousto-optics is able create AO filters with the passband required to separate individual optical channels in CWDM and DWDM systems [17]–[19]. However, the presence of the transmission function side lobes enables the radiation from the adjacent optical channels to pass partially through the AO filter.

The solution of this problem is either to increase the AO filters spectral resolution tenfold, or to develop some methods to suppress the transmission function side lobes. There are several papers devoted to the side lobes suppression but the methods outlined in these works are not very effective and significantly complicate the AO filtration system [20]–[22]. As for the substantial increase in the spectral resolution, its values indicated in [23] are limiting. So significant spectral resolution enhancement applying methods of conventional acousto-optics is very difficult.

In this paper we consider how the introduction of an optoelectronic feedback loop affects the operation and characteristics of the collinear AO filter and what additional possibilities for controlling the optical radiation spectral composition appear in this case. The results of the similar system study presented earlier in [24]–[27] has shown that changing the feedback parameters it is possible to control the width of the AO filter transmission function and suppress its side lobes.

It should be noted that AO devices with feedback [28]–[34] are the separate and poorly studied class of optoelectronic devices, which allows expanding significantly the range of optical tasks that can be solved with the use of acousto-optic interaction. The feedback appearance allows not only to improve the characteristics of already known AO devices, but also to create absolutely new AO devices [28]–[30], [33].

The feedback is realized by registration a part of the light radiation intensity at the output of the AO cell by a separate photodetector, the electrical signal from which controls either the frequency or the amplitude of the acoustic wave excited in the AO cell. The feedback introduction causes the appearance of different operating modes of AO devices, including bistable and chaotic [35]–[39]. The analysis of such devices operation is rather complicated. However, the prospects opened by the introduction of feedback in AO systems are so great that, of course, this area requires the detailed examination.

2. Basic Relations

The operation of the examined system is based on the effect of light radiation intensity modulation at the AO filter output with the frequency of ultrasound excited in it. This effect was predicted, described and theoretically studied in [40], [41]. Such a modulation is realized for the collinear AO interaction geometry [42], [43] as the wave vectors of the incident and diffracted light beams, as well as the wave vector of the ultrasound, are collinear. Thus, the key element of the system is the collinear AO filter. In our case it is made of a calcium molybdate crystal.

The incident and diffracted light beams propagate along one direction but have mutually orthogonal polarizations, as the collinear AO interaction is accompanied by the change of light polarization (anisotropic AO interaction). Thus in the common case the collinear AO cell is placed between two polarizers with orthogonal polarization planes to separate the incident and diffracted light beams. It was shown in [40], [41] that the regime in which the diffracted light beam intensity modulation arises is possible with a specific mutual orientation of the polarizer and analyzer polarization planes.

In the general case of incident optical radiation arbitrary polarization and the polarization plane of the input polarizer α, the light radiation at the AO cell output will consist of four components polarized along the crystallographic axes of the Z and Y crystal:

$$E_0^Y = E_i \cos\alpha \cdot \left(\cos\frac{A}{2} - j\frac{R}{2}\operatorname{sinc}\frac{A}{2\pi}\right) \cdot \exp\left[j\left(\omega_0 t - k_o l + \frac{R}{2}\right)\right] \tag{1}$$

$$E_{+1}^Z = -E_i\frac{\Gamma}{2}\cos\alpha \cdot \operatorname{sinc}\frac{A}{2\pi} \cdot \exp\left[j\left((\omega_0 + \Omega)\, t - k_e l - \frac{R}{2}\right)\right] \tag{2}$$

$$E_0^Z = E_i \sin\alpha \cdot \left(\cos\frac{A}{2} + j\frac{R}{2}\mathrm{sinc}\frac{A}{2\pi}\right) \cdot \exp\left[j\left(\omega_0 t - k_e l - \frac{R}{2}\right)\right] \tag{3}$$

$$E_{-1}^Z = E_i \frac{\Gamma}{2} \sin\alpha \cdot \mathrm{sinc}\frac{A}{2\pi} \cdot \exp\left[j\left((\omega_0 - \Omega)\, t - k_o l + \frac{R}{2}\right)\right] \tag{4}$$

Here $\Gamma = (2\pi/\lambda) l \Delta n$ is the Raman–Nath parameter (AO coupling coefficient) proportional to the acoustic wave amplitude aroused in the AO cell, Δn is the maximal change of the crystal refractive index under the action of the acoustic wave, l– AO interaction length, $R = (2\pi l/V)(f - V(n_e - n_o)/\lambda)$ is the dimensionless AO phase mismatch, $V = 2.9 \cdot 10^5$ cm/s is the velocity of the acoustic wave involved in the AO interaction (the calcium molybdate crystal was used), n_e and n_o are the refraction indices, λ is the optical wavelength, $A = \sqrt{\Gamma^2 + R^2}$, α - the polarizer polarization plane orientation with regard to the Y crystallographic axis of the AO cell crystal, $\Omega = 2\pi f$ is the frequency of ultrasound wave.

Passing through the output polarizer with a polarization plane oriented at an angle β to the Y crystallographic axis, they will acquire the same polarization and interfere. In the general case, the intensity of the light beam at the analyzer output can be written as the sum of three components with amplitudes depending on the mutual orientation of the polarizers:

$$I_d = I_0 + I_1 \cos(\Omega t + \phi_1 + \Phi) + I_2 \cos(2\Omega t + \phi_2 + 2\Phi) \tag{5}$$

where ϕ is the additional phase shift appearing at collinear AO interaction and Φ is acoustic wave phase.

In the conventional variant of AO collinear filter [42], [43], the incident light polarization is chosen in accordance with the crystal eigenmode polarizations (polarization angle α is equal to 90° or 0° with regard to the Y axis. Therefore, crossed analyzer (polarization angle β is equal to 0° or 90°, respectively) let pass only the diffracted optical radiation. In this case I_0 component that we will call constant component acquires maximal magnitude:

$$I_0 = I_i \frac{\Gamma^2}{4} \mathrm{sinc}^2\left(\frac{A}{2\pi}\right) \tag{6}$$

Simultaneously the I_1 and I_2 components equal zero. $I_0 = 1$ if $\Gamma = \pi$ and $R = 0$. Component I_1 we call it the first harmonic, reaches the maximum amplitude for α equal to 0 or 45 degrees and β equal to 45 and 90 degrees respectively ($I_0 = I_i/2$ at this geometry). First harmonic dependence on system parameters and time is described by the following equation:

$$I_1(t) = I_i \frac{\Gamma}{\Gamma^2 + R^2} \sin\left(\frac{A}{2}\right) \cdot \sqrt{4\cos^2\left(\frac{A}{2}\right) + R^2 \mathrm{sinc}^2\left(\frac{A}{2\pi}\right)} \cdot \cos(\Omega t + \phi_1 + \Phi) \tag{7}$$

A distinctive feature in this case is that the light radiation intensity will vary in time with the ultrasound frequency Ω excited in the AO cell. The first harmonic magnitude achieves maximal value when $\Gamma = \pi/2$. It should be noted that the optical signal at the analyzer output will always contain not only I_1 component but also a half of the input optical beam intensity. So it is not convenient to use it for the optical radiation filtration applications. The maximum of the component I_2 (so called second harmonic) will be achieved for $\alpha = \beta = 45$ degrees. If I_2 component is used, the light radiation intensity on the system output will be modulated in time with doubled ultrasound frequency.

The most interesting case of polarizer and analyzer mutual orientation takes place when I_1 component magnitude is maximal, since the presence of a light radiation intensity modulation with an ultrasound frequency makes it possible to create a feedback circuit in which the I_1 component is detected by a photodetector and the signal from the photodetector passes through amplifiers and feeds the AO cell transducer.

In the previous papers devoted to the examination of this system [28]–[31], the influence of feedback on its functioning and characteristics was studied only for the first harmonic.

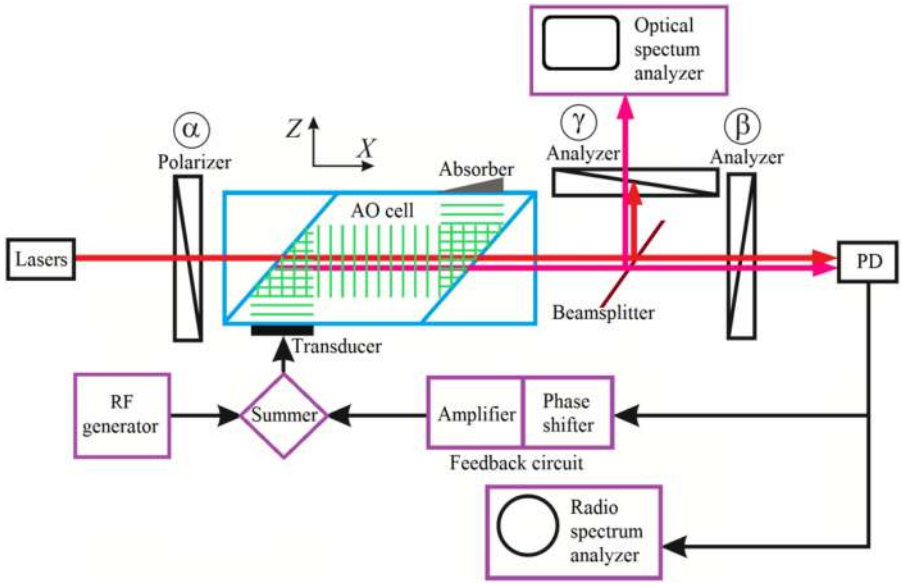

Fig. 1. The principal scheme of the examined optoelectronic system.

In this paper, we will consider how the feedback signal, created with the use of the first harmonic, affects the constant component that is used for AO filtration.

3. Examined System Description

The principal scheme of the examined AO system is shown in Fig. 1. The basic element of the setup is the collinear AO filter fabricated from calcium molybdate crystal [43] with 4 cm AO interaction length. The cell is placed between a polarizer and analyzers that specify the polarization of light at angles α, β and γ with regard to the crystallographic Y-axis.

A distinctive feature of this AO system from the previously examined [24]–[27] is that the beamsplitter is mounted before of the output polarizers. The polarization plane of the input polarizer is oriented orthogonally to Y crystallographic axis.

Such beamsplitter location allows us to divide the light beam on the output of the AO cell into two with polarizations controlled independently. One of the light beams passes through the analyzer with the polarization plane orthogonal ($\gamma = 0°$) to the input polarizer polarization plane. Such polarization planes mutual orientation corresponds to the standard application of collinear AO cells when they are placed between crossed polarizers to separate the diffracted light beam from the incident one [42], [43]. This optical beam will carry useful information, so let's call it signal. The second beam will pass through the analyzer, with the polarization plane oriented at an angle $\beta = 45°$ to the Y axis (the case of maximal I_1 component). Thus, its intensity will be modulated by amplitude with the ultrasound frequency, excited in the AO cell [24]–[27], [33], which makes it possible to use it for signal generation at the feedback circuit input, so we will call it the feedback beam.

The ThorLabs CPS635R module with 635 nm optical radiation wavelength or 633 nm He-Ne laser were used as the light sources. The feedback beam is registered by the Thorlabs PDA-10A photodetector connected to the input of the feedback circuit. The circuit includes phase shifter Mini-Circuits JSPHS-51+ and a pair of amplifiers Mini-Circuits ZHL-5W and ZFL-1200G+ that allows to tune the feedback circuit gain κ over a wide range.

The signal from the feedback output feeds the piezoelectric transducer of the AO cell. Oscilloscope or RF signal spectrum analyzer may be connected to the feedback circuit for the visualization and analysis of the feedback signal characteristics.

4. Basic Relations

In the previous studies considering only the feedback beam it was shown that the system has several operating modes depending on the feedback gain factor κ magnitude [24], [25]. At relatively low gain values, the system behave like a conventional AO filter - the central transmission wavelength can be tuned by varying the RF generator frequency. In this case, the shape of the transmission function and the AO interaction efficiency will be determined by the feedback gain. The effect of the feedback circuit presence is the greater, the greater is κ and less the amplitude of the RF generator signal. For large κ values, the system may exceed the self-excitation threshold and become an optoelectronic generator [29]. In this case a separate RF generator will no longer be needed for its operation and the spectrum of the electrical signal in the feedback circuit will be determined by the spectrum of optical radiation at the AO filter input.

4.1 Single Spectral Component

Let's assume that the input optical radiation contains only one spectral component. This will help us to determine the examined system transmission function and its transformation under the action of the feedback signal. The polarizer and feedback beam analyzer are oriented so that the amplitude of the first harmonic is maximal ($\alpha = 0°$, $\beta = 45°$). Then the intensity of the optical beam used in the feedback circuit at the output of the analyzer will be described by the following equation.

$$\begin{aligned} I_d(t) &= \vartheta\left(I_0 + I_1\cos(\Omega t + \phi_1 + \Phi)\right) \\ &= \frac{I_i\vartheta}{2}\left\{1 + \frac{\Gamma}{2}\mathrm{sinc}\left(\frac{A}{2\pi}\right)\cdot\sqrt{4\cos^2\left(\frac{A}{2}\right) + R^2\mathrm{sinc}^2\left(\frac{A}{2\pi}\right)}\cdot\cos(\Omega t + \phi_1 + \Phi)\right\} \end{aligned} \tag{8}$$

where I_i - is the incident light intensity, and ϑ is the beamsplitter ratio (the 50:50 Thorlabs EBS2 beamsplitter was used in experiment).

When the AO phase matching condition is fulfilled $R = 0$ and $I_1 = (I_i/2)\sin\Gamma$. The amplitude I_1 achieves maximal value 0.5 at the Raman-Nath value $\Gamma = \pi/2$. In this case the output intensity changes harmonically in time with the frequency of ultrasound Ω from zero to the intensity of the incident light I_i. This is the only case in the acousto-optics when AO cell produces 100% amplitude modulation of the optical beam intensity not after the diffraction on the standing acoustic wave but on the travelling acoustic wave.

The additional phase shift ϕ_1 appearing at collinear AO interaction is defined by the equation:

$$\tan\varphi_1 = \frac{A}{R}\cot\left(\frac{A}{2}\right) \tag{9}$$

In the case when phase matching condition is fulfilled (R = 0) $\phi_1 = \pi/2$

If we neglect the constant term $I_i\vartheta/2$ in Eq. (8) as it doesn't influence the acoustic wave magnitude. The RF signal on the transducer may be described by the following equation:

$$U(t) = U_g\cos(\Omega t) + \sigma\kappa\vartheta I_i\frac{\Gamma}{4}\mathrm{sinc}\left(\frac{A}{2\pi}\right)\cdot\sqrt{4\cos^2\left(\frac{A}{2}\right) + R^2\mathrm{sinc}\left(\frac{A}{2\pi}\right)}\cdot\cos(\Omega t + \phi_1 + \Phi + \chi) \tag{10}$$

here, U_g is the amplitude of harmonic oscillations of the RF generator, σ - is the sensitivity of the photodetector, κ - is the gain factor of the amplifier, and χ - is the phase shift produced by the phase shifter. The sum of Eq. (10) terms will be maximal if:

$$\chi = -\phi_1 \tag{11}$$

This equation indicates that the phase shifter has to compensate the AO phase shift ϕ_1. In the experiment we don't adjust the phase shifter when the ultrasound frequency is tuned, so the X value is set to be -0.5π in accordance with Eq. (9).

The acoustic wave phase Φ is described by the following equation:

$$\tan\Phi = \frac{\sigma\kappa\vartheta I_1 \sin(\Phi+\chi+\phi_1)}{U_g + \sigma\kappa\vartheta I_1 \cos(\Phi+\chi+\phi_1)} - R \tag{12}$$

It is possible to rewrite Eq. (10) as:

$$U(t) = U_0 \cos(\Omega t + \Phi) \tag{13}$$

where U_0 is the following:

$$U_0 = \left\{ U_g^2 + \left(\sigma\kappa\vartheta I_i \frac{\Gamma}{4} \mathrm{sinc}\left(\frac{A}{2\pi}\right) \cdot \sqrt{4\cos^2\left(\frac{A}{2}\right) + R^2 \mathrm{sinc}^2\left(\frac{A}{2\pi}\right)} \right)^2 + 2U_g \sigma\kappa\vartheta I_i \frac{\Gamma}{4} \mathrm{sinc}\left(\frac{A}{2\pi}\right) \cdot \right.$$
$$\left. \cdot \sqrt{4\cos^2\left(\frac{A}{2}\right) + R^2 \mathrm{sinc}^2\left(\frac{A}{2\pi}\right)} \cos(\Phi+\phi_1+\chi) \right\}^{1/2} \tag{14}$$

The Raman–Nath parameter Γ is proportional to the acoustic wave amplitude and, consequently, to the electrical voltage amplitude U_0 applied to the transducer:

$$\Gamma = \mu U_0 \tag{15}$$

where μ - is transformation the coefficient determined by characteristics of the transducer and the AO cell. After measuring the SWR (standing wave ratio) of the AO cell we by vector network analyzer will consider μ to be as high as 0.9.

Eqs. (12) and (15) form the phase and magnitude balance conditions for the examined system. Solving this system of equations it is also possible to define the dependence of AO diffraction efficiency on the mismatch for the signal beam, or in other words to define the transmission function of the system for the signal optical beam:

$$I_d = I_i(1-\vartheta) \cdot \frac{\Gamma^2(R,\Phi)}{4} \cdot \mathrm{sinc}^2\left(\frac{A(R,\Phi)}{2\pi}\right) \tag{16}$$

where R and Φ are defined from Eqs. (12) and (15).

4.2 Two Spectral Components

Let's assume that the input optical radiation contains several discrete spectral components. This will help us to determine the spectral resolution of the examined system and to define the system parameters for the applications in WDM systems. Let's pretend that the optical radiation containing two optical wavelengths λ_1 and λ_2 passes through the examined system. Than I_{11} is the first harmonic intensity at λ_1 wavelength and I_{12} is the first harmonic intensity at λ_2 wavelength. Both feedback beams intensities I_{d1} and I_{d2} will be defined by the equations similar to Eq. (8):

$$I_{d1}(t) = \vartheta(I_{01} + I_{11}\cos(\Omega t + \phi_1 + \Phi))$$
$$= \frac{I_{i1}\vartheta}{2}\left\{1 + \frac{\Gamma}{2}\mathrm{sinc}\left(\frac{A_1}{2\pi}\right) \cdot \sqrt{4\cos^2\left(\frac{A_1}{2}\right) + R_1^2\mathrm{sinc}^2\left(\frac{A_1}{2\pi}\right)} \cdot \cos(\Omega t + \phi_1 + \Phi)\right\} \tag{17}$$

$$I_{d2}(t) = \vartheta(I_{02} + I_{12}\cos(\Omega t + \phi_2 + \Phi))$$
$$= \frac{I_{i2}\vartheta}{2}\left\{1 + \frac{\Gamma}{2}\mathrm{sinc}\left(\frac{A_2}{2\pi}\right) \cdot \sqrt{4\cos^2\left(\frac{A_2}{2}\right) + R_2^2\mathrm{sinc}^2\left(\frac{A_2}{2\pi}\right)} \cdot \cos(\Omega t + \phi_2 + \Phi)\right\} \tag{18}$$

where $A_1 = \sqrt{\Gamma^2 + R_1^2}$, $A_2 = \sqrt{\Gamma^2 + R_2^2}$, R_1 and R_2 are the AO mismatches for wavelengths λ_1 and λ_2.

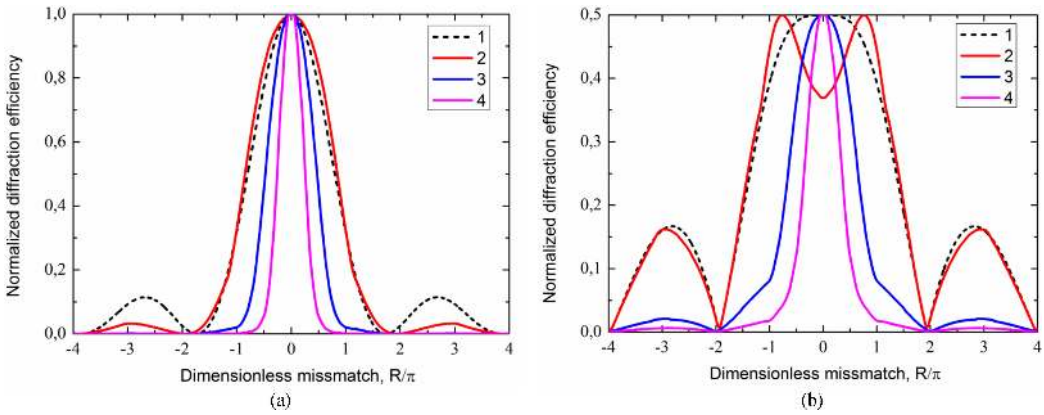

Fig. 2. The AO filter transmission functions transformation for the signal optical beam (a) and feedback beam (b). Curve 1 -$\kappa = 0$; Curve 2 - $\kappa = 6.3$, $\Gamma_g = \pi/2$; Curve 3 - $\kappa = 6.3$, $\Gamma_g = \pi/20$; Curve 4 - $\kappa = 6.3$, $\Gamma_g = \pi/200$.

In the same way as for Eq. (10) the RF signal feeding the AO cell transducer will be:

$$U(t) = U_g \cos(\Omega t) + \sigma\kappa\vartheta I_{i1}\frac{\Gamma}{4}\mathrm{sinc}\left(\frac{A_1}{2\pi}\right)\cdot\sqrt{4\cos^2\left(\frac{A_1}{2}\right) + R_1^2\mathrm{sinc}^2\left(\frac{A_1}{2\pi}\right)}\cdot\cos(\Omega t + \phi_1 + \Phi + \chi) +$$

$$+\sigma\kappa\vartheta I_{i2}\frac{\Gamma}{4}\mathrm{sinc}\left(\frac{A_2}{2\pi}\right)\cdot\sqrt{4\cos^2\left(\frac{A_2}{2}\right) + R_2^2\mathrm{sinc}^2\left(\frac{A_2}{2\pi}\right)}\cdot\cos(\Omega t + \phi_2 + \Phi + \chi) \quad (19)$$

It is possible to neglect the constant terms in Eq. (19) as they don't influence the acoustic wave magnitude. So this equation will transform into:

$$U(t) = U_0 \cos(\Omega t + \delta) \quad (20)$$

where U_0 value is defined by:

$$U_0 = \left\{U_g^2 + 2\sigma\kappa U_g\left(I_{11}\cos(\phi_1 + \Phi + \chi) + I_{12}\cos(\phi_2 + \Phi + \chi)\right)\right.$$

$$\left.+\sigma^2\kappa^2\left(I_{11^2+I_{12}^2}\right) + 2\sigma\kappa I_{11}I_{12}\cos(\phi_1 - \phi_2)\right\}^{1/2} \quad (21)$$

and phase equals:

$$\tan\delta = \frac{\sigma\kappa\{I_{11}\sin(\phi_1 + \Phi + \chi) + I_{12}\sin(\phi_2 + \Phi + \chi)\}}{U_g + \sigma\kappa\{I_{11}\cos(\phi_1 + \Phi + \chi) + I_{12}\cos(\phi_2 + \Phi + \chi)\}} \quad (22)$$

The additional phase shift χ introduced by phase shifter is constant and equals -0.5π.

5. Experimental and Simulation Results

5.1 Single Spectral Component

5.1.1 Simulation Results: Let us suppose that the light radiation on the optical input of the examined system contains only one spectral component. The mathematical model of the system for such case was presented in subsection 4.1. Let us consider how the feedback circuit gain value and the RF generator signal amplitude affects the feedback signal and collinear AO filtering characteristics for the signal light beam. Figure 2 represents the AO diffraction efficiency $\varsigma = I_d/I_i$ dependences for both optical beams on AO mismatch R magnitude (transmission functions) simulated for various values of AO system parameters (feedback gain κ and Raman-Nath parameter Γ, proportional to the acoustic wave magnitude aroused in the AO cell). The $I_0(R)$ dependences show the collinear AO filtering characteristics. The $I_1(R)$ dependences characterize the change in

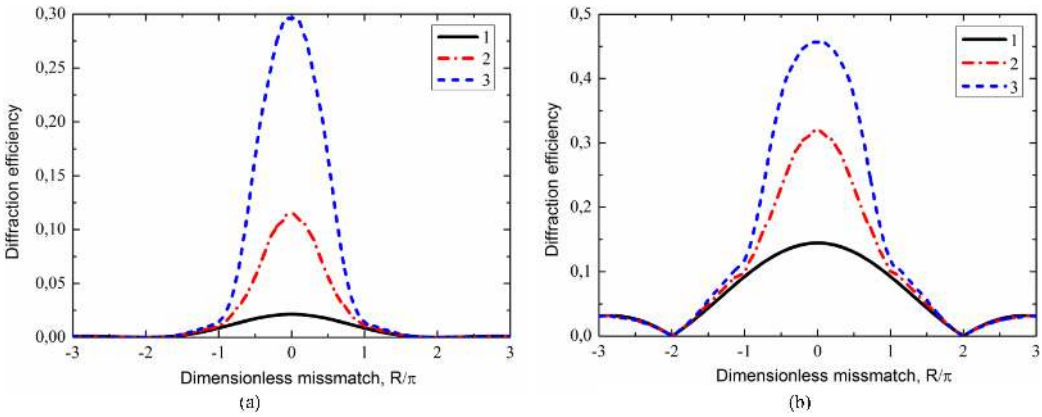

Fig. 3. The AO filter transmission functions transformation for the signal optical beam (a) and feedback beam (b) for the Raman-Nath parameter value $\Gamma_g = \pi/10$ and various feedback gain magnitudes; Curve 1 -$\kappa = 0$; Curve 2 - $\kappa = 4$; Curve 3 - $\kappa = 6$.

feedback circuit signal amplitude as a function of R magnitude and, consequently, the amplitude of the acoustic wave in the AO cell. Since the signal amplitude U_g fed from the RF generator does not depend on the ultrasound frequency.

The $I_0(R)$ and $I_1(R)$ dependences transformation obtained for $\kappa = 6.3$ and varying Raman-Nath parameter magnitudes is represented in Fig. 2a and Fig. 2b correspondingly. Such feedback gain value is slightly less than system excitation threshold [21], [22]. The dashed curves 1 in Fig. 2a and 2b represent the $I_0(R)$ and $I_1(R)$ dependences when the feedback is absent for the case of maximal diffraction efficiency ($\Gamma_g = \mu U_g = \pi$ for $I_0(R)$ in Fig. 2a and $\Gamma_g = \pi/2$ for $I_1(R)$ in Fig. 2b).

Curves 2-4 were obtained for $\kappa = 6.3$ and $\Gamma_g = \pi/2$, $\Gamma_g = \pi/20$ and $\Gamma_g = \pi/200$ correspondingly. The normalized to the maximum AO interaction efficiency is postponed along the vertical axis in both figures.

The presented calculations results show that the feedback influence is the greater the smaller is the amplitude of the signal fed from the RF generator. The decrease of the generator signal magnitude leads to the system bandwidth narrowing and the transmission function side lobes suppression.

An interesting point is that in the presence of feedback when $\Gamma_g = \pi/2$ the overmodulation is observed for $I_1(R)$ (Fig. 2b, curve 2). This means that the AO diffraction efficiency for the phase matching case ($R = 0$) is lower than maximal possible. The overmodulation causes the $I_1(R)$ function half-width broadening about 4% and consequently the $I_0(R)$ transmission function passband increases also about 4%. The $I_0(R)$ function side lobes decrease in this case approximately in 3.5 times in comparison with transmission function without feedback. The side lobes suppression positively affects the AO filter spectral contrast ε and its real spectral resolution. The spectral contrast we will define as the ratio of the AO filter transmission function main and first side maxima values.

The $I_1(R)$ half-width reduces in 2.1 times and $I_0(R)$ - in 1.7 times when the Raman-Nath parameter decreases till $\Gamma_g = \pi/20$. At the same time, the spectral contrast increases to 720 versus 8.7 for the same filter without feedback. It should be noted that all these transformations are accompanied by the AO interaction efficiency decrease, so, if $\varsigma = 0.84$ for the curve 2 in Fig. 2a then $\varsigma = 0.23$ for the curve 3. A further decrease in the Raman-Nath parameter ($\Gamma_g = \pi/200$ - curve 4 in Fig. 2a) leads to an even narrower passband (in 3 times) and spectral contrast enhancement $\varepsilon = 6750$ while the half-width of the signal in the feedback $I_1(R)$ decreases by a factor of 4.

Figure 3 shows the AO diffraction efficiency calculations results for both output light beams on AO mismatch R magnitude for a fixed value of the Raman-Nath parameter equal to $\pi/10$ (that corresponds 100 times lower RF generator signal power than needed to obtain $\varsigma = 1$) and various feedback gain values ($\kappa = 0$ - curve 1, $\kappa = 4$ - curve 2 и $\kappa = 6$ - curve 3).

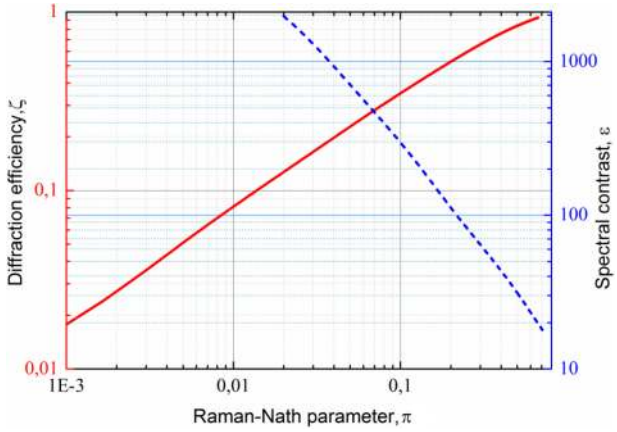

Fig. 4. The alteration of the AO interaction efficiency (solid curve) and the AO filter spectral contrast (dotted curve) as a function of the Raman-Nath parameter Γ_g value.

The presented dependences illustrate that, the AO interaction efficiency grows and the transmission function bandwidth decreases as the gain increases. In this case the change in κ magnitude does not affect the side lobes in any way.

The diffraction efficiency increase in 14 times for the I_0 component with κ growth from zero to 6. Its passband reduces in 1.7 times. The I_1 component behavior was studied in details in [29]–[31]. The spectral contrast of the examined collinear AO filter equals 21 when $\kappa = 0$ if $\Gamma_g = \pi/10$. If the feedback coefficient increases till $\kappa = 6$ the spectral contrast will be as high as 290 for the same Γ_g value. So adding the feedback we may control effectively the shape of collinear AO filter transmission function.

The AO interaction efficiency $\varsigma$and the spectral contrast ε dependences on the Γ_g parameter value calculated for $\kappa = 6.3$ are shown in Fig. 4. The range of the Raman-Nath parameter variation in the presented figure lies between $\pi/\sqrt{2} \leq \Gamma_g \leq \pi/1000$. As noted earlier, the AO interaction efficiency decreases from 1 to 0.017 with Γ_g decreasing, and the spectral contrast, calculated in the range $\pi/\sqrt{2} \leq \Gamma_g \leq \pi/50$, increases from 20 to almost 2000.

Thus, the application of feedback leads to a significant decrease of the AO filter transmission function side lobes and enhancement of its real spectral resolution, but is accompanied by a decrease in the AO interaction efficiency.

5.1.2 Experimental Results: The simulation results presented above were verified experimentally. In the experiment the $I_0(f)$ and $I_1(f)$ dependences were registered by oscilloscope while the RF generator was operating in the sweep mode. Here it should be mentioned that as the dimensionless variables are used in theoretical model (especially the incident optical beam normalized intensity $I_i = 1$), the theoretical gain coefficients doesn't match with the experimental ones. The results of the measurements are represented in Fig. 5.

The I_0 component was measured by oscilloscope channel 1 (yellow curve) and I_1 – by channel 2 (purple curve) simultaneously, the horizontal and vertical scale is the same for all figures. All figures were obtained for RF generator signal amplitude 5V. The Fig. 5a corresponds to the case when there is no feedback $\kappa = 0$, $\kappa = 85$ for Fig. 5b and 190 for Fig. 5c. The same transformation of the transmission functions shape is observed as it was predicted and illustrated by Fig. 3. We may also notice that the side lobes magnitude is being set only by the RF generator magnitude while the main maximum height depends on the feedback gain in the full correspondence with theoretical predictions.

The results of this experiment are summarized in Fig. 6 where the I_0 transmission function passband narrowing and AO diffraction efficiency dependences on RF generator acoustic power obtained for three various gain values are presented. The highest I_0 transmission function

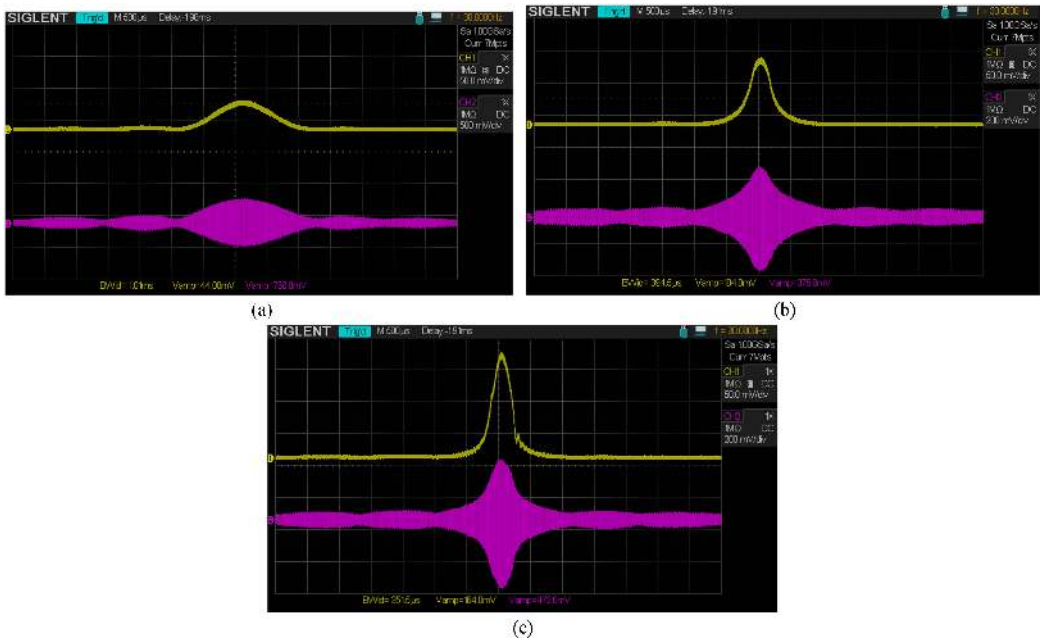

Fig. 5. The collinear AO filter transmission functions for I_0 and I_1 components without (a) and in the presence of feedback (b), (c).

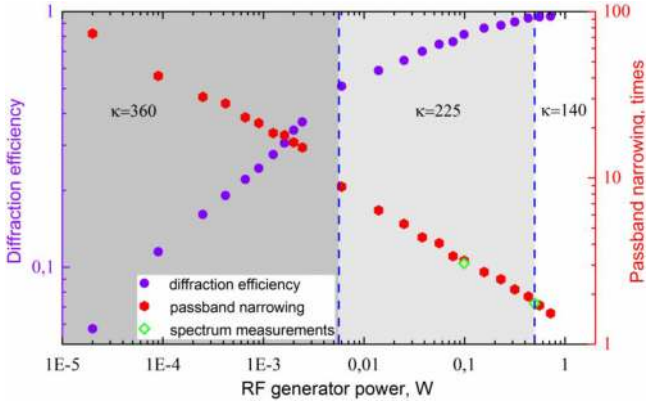

Fig. 6. The dependences of AO diffraction efficiency (1) and collinear AO filter transmission function passband narrowing (2) on RF generator acoustic power.

narrowing that was observed experimentally was 74 times, unfortunately as for I_1 component [24] the narrowing is accompanied by the decrease of AO diffraction efficiency from 95% till 6%.

Rhombuses in the figure 6 indicate the parameters of the system where the spectrum of the output signal beam was measured (curves *3* and *4* in Fig. 7).

The effect of the feedback gain value on the AO filter passband was not only measured by examination of transmission function transformation, but also checked by the observation of optical radiation spectrum composition alteration when passing through the system. The laser module ThorLabs CPS635R spectrum which has a fairly wide radiation band was used in this experiment. The results of these spectral measurements are shown in Fig. 7. The signal optical beam spectrum was measured for the several cases. In the first variant optical radiation passed through the system but the acoustic wave was not excited in the AO cell so the diffraction was absent, the polarization planes of the input polarizer and the signal optical beam analyzer were set to be parallel (so the

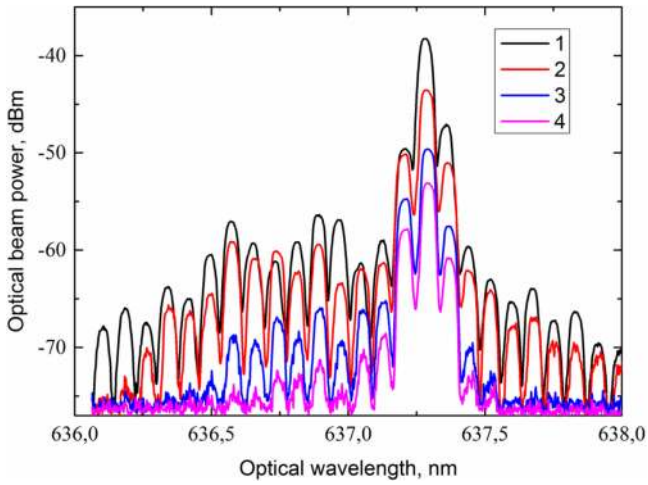

Fig. 7. The optical radiation spectra at the output of the examined AO system in the following cases: 1 – laser module spectrum; 2 – conventional collinear AO filter, RF generator power 3W; 3 – collinear AO filter with feedback, $\kappa = 225$, RF generator power 0.5W; 4 – collinear AO filter with feedback, $\kappa = 225$, RF generator power 0.1W.

own optical radiation spectrum of the module was measured). The results of such a measurement are shown by curve *1* in Fig. 7.

In the second variant (curve *2*), the spectrum of the signal optical beam was measured in the case when $\kappa = 0$ (usual collinear AO filter) and 3W RF generator acoustic power. In the third case, the gain of the feedback was equal to 225, and the RF generator signal power was 0.5 W. The observed narrowing of the AO system passband measured with an oscilloscope was 1.8 times, the optical radiation spectrum of the signal light beam in this case is illustrated by curve *3*. In the fourth case, the gain was also equal to 225, but the RF generator signal power was reduced to 0.1W, in this case the system passband reduced more than in 3 times, and the optical radiation at the system output has the spectrum illustrated by curve *4*.

Comparing the presented spectra, it is possible to make the following conclusions. Since the collinear AO filter used for measurements has a 0.9 nm passband, the effect of its selectivity could be noticed only near the borders of the presented spectral range (optical modes of the laser with wavelengths of about 636 nm are suppressed for the curve *2* in comparison with curve *1*). The introduction of the feedback allows us to narrow significantly the passband and suppress the side lobes of the transmission function. So the spectral composition of the optical radiation at the system output changes significantly – only modes with wavelengths in the range from 636.5 to 637.5 nm remain. Thus, the full system bandwidth is reduced to 1 nm. Reducing the power of the RF generator signal by a factor of 5 (from 0.5W to 0.1W) in the presence of feedback causes the full transmission band narrowing to about 0.5 nm. The observed narrowing is in full accordance with the results of calculations and measurements presented above.

Thereby the change of the feedback circuit parameters and the RF generator power makes it possible to control the optical radiation spectral composition at the output of the examined AO system that is, to perform AO spectral filtering with adjusted transmission function passband.

5.2 Two Spectral Components

5.2.1 Simulation Results: Let's consider now the case when optical radiation at the system input contains several spectral components. We assume for simplicity that the optical radiation contains two spectral components. This is enough to determine the spectral resolution of the system and to examine the influence of the feedback on it. The mathematical model for such situation was presented in section 4.2 of this paper.

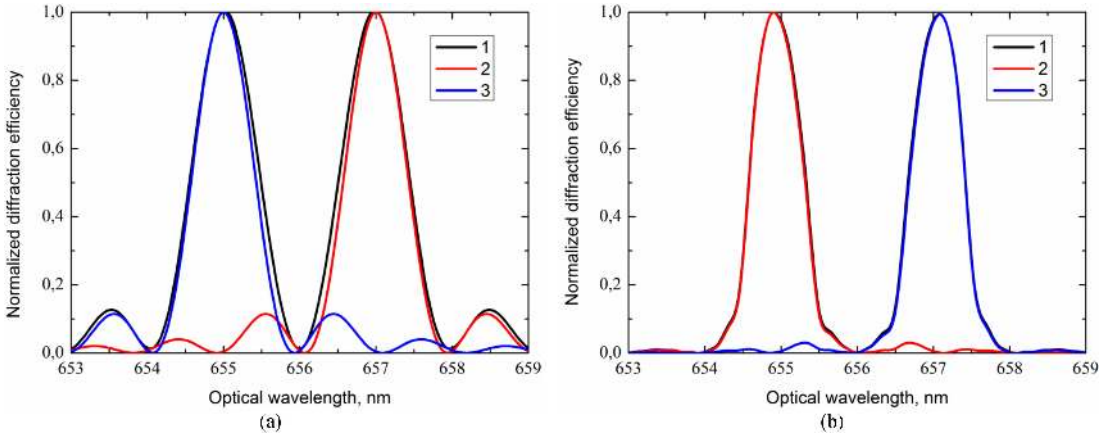

Fig. 8. Examined system optical response on the incident light with two spectral components $\lambda_1 =$ 655 nm and $\lambda_2 = 657$ nm without (a) and with (b) feedback; Curve 1 - full response; Curves 2 and 3 – response for each spectral component.

Let's consider at first the case when the optical beam at the system input contains two spectral components with wavelengths $\lambda_1 = 655$ nm and $\lambda_2 = 657$ nm of equal intensity. Thus, $\Delta\lambda = 2$ nm, that exceeds more than twice the AO filter passband. The results of system response calculations are shown in Fig. 8. Curves 1 in Fig. 8 illustrate the full response to both wavelengths, curves 2 and 3 – for each spectral component. Fig. 8a illustrates the case when the feedback is absent. In this case, the AO filter transmission functions corresponding to the optical spectrum components overlap near the first minimum, however, the first and second side lobes are almost completely inside the main maximum of the adjacent wavelength. This means that part of the light intensity from one spectral component will pass through the AO filter at diffraction of adjacent spectral component. It is necessary either to reduce the filter passband (this can be realized either by increasing the AO interaction length, or by choosing a geometry of the AO diffraction and AO cell material that will provide a higher frequency of the AO synchronism), or to enlarge $\Delta\lambda$ between the incident light spectral components to reduce this negative effect in conventional acousto-optics, and this is not acceptable for fiber-optic communication lines as the channel spacing is fixed.

Fig. 8b presents the calculations results for the case when the feedback gain is $\kappa = 6.3$, and $\Gamma_g = \pi/5$ (which corresponds to 25 times lower acoustic power then required to achieve 100% diffraction efficiency in the absence of feedback). In this variant the transmission functions overlap also at about the first minimum, but due to a larger spectral contrast (34 versus 8.7 for the case without feedback), the light energy of the adjacent optical channel that passes through the filter is 10 times less than in case when there is no feedback. Thus, introducing feedback, it is possible to reduce significantly the mutual impact between adjacent spectral channels without changing the AO cell design. A negative effect in this case will be an increase in optical losses in the system, since such choice of the optoelectronic system parameters provides only 50% AO interaction efficiency.

If we reduce $\Delta\lambda$ to 1.3 nm – due to the specificity of the feedback signal generation [30], this value of the spectral interval turns out to be limiting in theoretical calculations for the system with collinear AO filter and feedback. In this case for conventional collinear filter (Fig. 9a) the transmission functions main maxima overlapping of adjacent spectral components will occur at about 20% of the maximum value. This is, of course, better than the Rayleigh criteria but is poorly applicable for operation in optoelectronic devices.

The introduction of feedback can improve the situation. Figure 9b represents the results of the system response simulations for $\Delta\lambda = 1.3$ nm, $\kappa = 6.3$ and various values of the Raman-Nath parameter: curve *1* - $\Gamma_g = \pi/25$, curve *2* - $\Gamma_g = \pi/50$ and curve *3* - $\Gamma_g = \pi/100$. The simulation shows that a decrease of Γ_g value and constant κ that is close to the system self-excitation threshold makes it possible to reduce the level at which the diffraction maxima corresponding to the adjacent

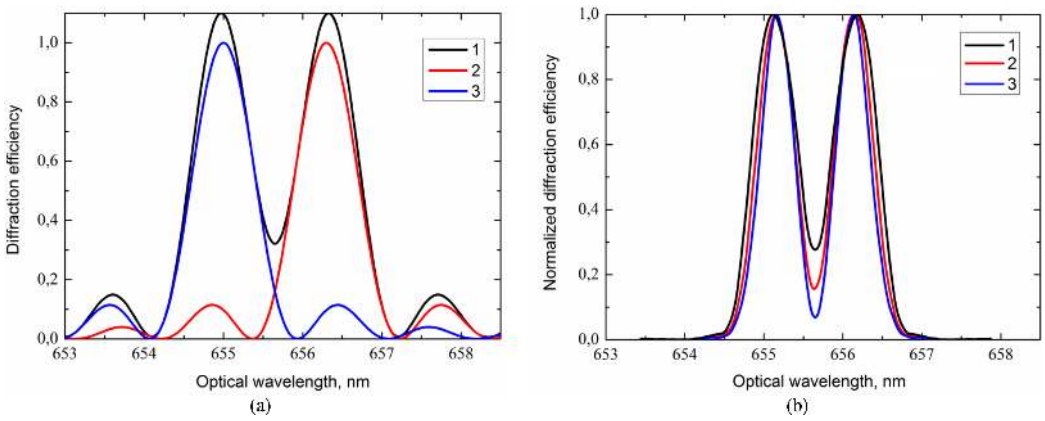

Fig. 9. Examined system optical response on the incident light with two spectral components $\lambda_1 =$ 655 nm and $\lambda_2 = 656.3$ nm without (a) and with (b) feedback $\kappa = 6.3$; (a)- curve 1 - full response; curves 2 and 3 – response for each spectral component. (b) - curve 1 - $\Gamma_g = \pi/25$; curve 2 - $\Gamma_g = \pi/50$; curve 3 - $\Gamma_g = \pi/100$.

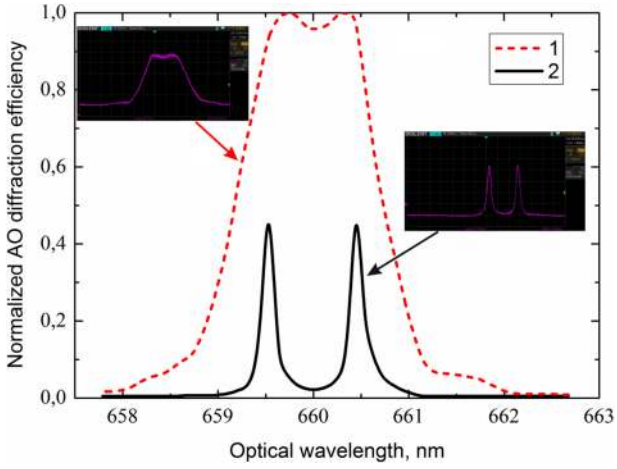

Fig. 10. The oscillograms of examined system transmission functions for the incident optical radiation with two spectral components $\Delta\lambda = 0.9$ nm; curve 1 - $\kappa = 0$, curve 2 - $\kappa = 590$.

spectral channels overlap due to the transmission function narrowing and spectral contrast increase. If $\Gamma_g = \pi/25$ the overlapping is observed at 28% of the maximum diffraction efficiency, then at $\Gamma_g = \pi/50$ it decreases to 16%, and with Γ decreasing to $\Gamma_g = \pi/100$, the transmission functions overlap already at the level of 7% of the maximum. It is possible to achieve an even greater reduction, up to almost zero, but this will be accompanied by too much loss in the AO interaction efficiency.

The results of the calculations were verified experimentally using two identical laser modules with a wavelength of about 655 nm. Laser modules radiated at almost identical wavelengths, heating one of them allowed tuning slightly its optical radiation wavelength. Fig. 10 represents the processed oscillograms of the examined AO system responses in the case when $\Delta\lambda$ was 0.9 nm. The optical radiation wavelength is postponed along the horizontal axis and normalized AO diffraction efficiency – along horizontal. The original oscillograms obtained when RF generator was operating in the sweep mode are also presented as the inserts. If there is no feedback (curve 1) then the collinear filter was hardly able to distinguish two wavelengths. The signal magnitude in the center of the presented transmission function is only 4% less than the maximal value. The observed dependences change significantly with the introduction of feedback (curve 2). It is possible to achieve almost complete absence of overlapping of the transmission functions of the adjacent spectral components in experiment. At the same time, the AO diffraction efficiency is reduced to

47%. The curve 2 shown in Fig. 10 was obtained for the feedback gain $\kappa = 590$. It should be noted that the results of the experimental study are better than the theoretical ones. So in the experiment, $\Delta\lambda = 0.9$ nm, is the limiting value of the spectral interval between the optical radiation spectrum components that may be distinguished by the examined system in the presence of feedback. This $\Delta\lambda$ corresponds to the passband of the AO filter used when there is no feedback, while the calculations give a limiting value equal to 1.3 nm.

Thus, the analysis of the presented results allows us to conclude that the introduction of feedback can substantially increase the real spectral resolution of the AO filter.

4. Conclusions

In this paper the examination of an optoelectronic system containing a collinear AO filter and a feedback circuit was continued. It was shown that introducing feedback it is possible to produce collinear AO filter with adjustable transmission function. The signal in the feedback circuit appears due to a separate photodetector on which a part of the output optical radiation intensity is directed. The difference between the investigated system and the previously studied ones is that a beam splitter is installed directly at the optical output of the AO filter. This modification allows dividing the output optical beam into two parts, one of which is used to excite the signal in the feedback circuit, and the second is used for filtration and carries useful signal. The effect of light intensity modulation that was discovered previously for the collinear geometry of AO interaction is applied to arouse the signal in feedback circuit. This effect appears when the special geometry of polarizers polarization planes mutual orientation between which the AO filter is located is being set. The polarization plane of the analyzer must be orthogonal to the polarization plane of the input polarizer in order to suppress light in the zero order of diffraction for a signal light beam, since this is done for the conventional case of collinear AO filtration.

The influence of the feedback circuit parameters and the external RF generator signal magnitude on the system optical characteristics was examined. The influence of the feedback signal on the system bandwidth and the AO interaction efficiency was evaluated and measured experimentally. It was shown that the introduction of feedback makes it possible to achieve a significant narrowing of the bandwidth (by a factor of 74) and an increase in the AO filter spectral contrast (by a factor of thousands), which makes it possible the enhancement of AO system real spectral resolution. It has been shown experimentally that in the presence of feedback, the AO system allows us to resolve confidently the spectral components of the optical radiation spaced 0.9 nm apart, while the same AO filter without feedback has a passband of the same width. The demonstrated effective suppression of the AO filter transmission function side lobes opens the way to apply the AO devices in fiber-optic communication systems, since it allows suppressing almost completely the illumination from the adjacent spectral channels

References

[1] J. Xu and R. Stroud, *Acousto-Optic Devices*. New York, NY, USA: Wiley, 1992.
[2] A. P. Goutzoulis and D. R. Pape, *Design and Fabrication of Acousto-Optic Devices*. New York, NY, USA: Marcel Dekker, 1994.
[3] Q. Liu, F. Lu, M. Gong, C. Li, and D. Ma, "15W output power diode-pumped solid-state lasers at 515nm," *Laser Phys. Lett.*, vol. 4, pp. 30–32, 2007.
[4] R. A. Sprague and C. L. Koliopoulos, "Time integrating acoustooptic correlator," *Appl. Opt.*, vol. 15, no. 1, pp. 89–92, 1976.
[5] K. B. Yushkov, V. Y. Molchanov, A. V. Ovchinnikov, and O. V. Chefonov, "Acousto-optic replication of ultrashort laser pulses," *Phys. Rev. A*, vol. 96, 2017, Art. no. 043866.
[6] D. A. Belyaev *et al.*, "Compact acousto-optic imaging spectro-polarimeter for mineralogical investigations in near infrared," *Opt. Exp.*, vol. 25, no. 21, pp. 25980–25991, 2017.
[7] O. I. Korablev, D. A. Belyaev, Y. S. Dobrolenskiy, A. Y. Trokhimovskiy, and Y. K. Kalinnikov, "Acousto-optic tunable filter spectrometers in space missions," *Appl. Opt.*, vol. 57, no. 10, pp. C103–C119, 2018.
[8] V. Leroi, J.-P. Bibring, and M. Berthe, "MicrOmega/IR: Design and status of a nearinfrared spectral microscope for *in situ* analysis of Mars samples," *Planet. Space Sci.*, vol. 57, pp. 1068–1075, 2009.

[9] J.-L. Bertaux *et al.*, "SPICAV/SOIR on Venus express: Three spectrometers to study the global structure and composition of the Venus atmosphere," *Planet. Space Sci.*, vol. 55, pp. 1653–1672, 2007.
[10] V. I. Balakshy and S. N. Mantsevich, "Influence of the divergence of a light beam on the characteristics of collinear diffraction," *Opt. Spectrosc.*, vol. 103, no. 5, pp. 804–810, 2007.
[11] S. N. Mantsevich and V. I. Balakshy, "Acousto-optic interaction in an inhomogeneous acoustic field," *Opt. Spectrosc.*, vol. 118, no. 4, pp. 617–622, 2015.
[12] S. N. Mantsevich, V. I. Balakshy, V. Y. Molchanov, and K. B. Yushkov, "Influence of acoustic anisotropy in paratellurite on quasicollinear acousto-optic interaction," *Ultrasonics*, vol. 63, pp. 39–46, 2015.
[13] S. N. Mantsevich, V. Y. Molchanov, K. B. Yushkov, V. S. Khorkin, and M. I. Kupreychik, "Acoustic field structure simulation in quasi-collinear acousto-optic cells with ultrasound beam reflection," *Ultrasonics*, vol. 78, pp. 175–184, 2017.
[14] S. N. Mantsevich, T. V. Yukhnevich, and V. B. Voloshinov, "Examination of the temperature influence on the acousto-optic filters performance," *Opt. Spectrosc.*, vol. 122, pp. 675–681, 2017.
[15] E. Dekemper, J. Vanhamel, B. Van Opstal, D. Fussen, and V. B. Voloshinov, "Influence of driving power on the performance of UV KDP-based acousto-optical tunable filters," *J. Opt.*, vol. 17, 2015, Art. no. 075404.
[16] V. P. Zarubin *et al.*, "Laser-ultrasonic temperature mapping of an acousto-optic dispersive delay line," *NDT Int.*, vol. 98, pp. 171–176, 2018.
[17] J. Sapriel, D. Charissoux, V. Voloshinov, and V. Molchanov, "Tunable acoustooptic filters and equalizers for WDM applications," *J. Lightw. Technol.*, vol. 20, no. 5, pp. 864–871, May 2002.
[18] V. Y. Molchanov, V. B. Voloshinov, and O. Y. Makarov, "Quasi-collinear tunable acousto-optic paratellurite crystal filters for wavelength division multiplexing and optical channel selection," *Quantum Electron.*, vol. 39, no. 4, pp. 353–360, 2009.
[19] J.-C. Kastelik, K. B. Yushkov, S. Dupont, and V. B. Voloshinov, "Cascaded acousto-optical system for the modulation of unpolarized light," *Opt. Exp.*, vol. 17, no. 15, pp. 12767–12776, 2009.
[20] D. A. Smith and J. J. Johnson, "Sidelobe suppression in an acousto-optic filter with a raised-cosine strength," *Appl. Phys. Lett.*, vol. 61, pp. 1025–1027, 1992.
[21] D. A. Smith and J. J. Johnson, "Two-stage integrated-optic acoustically tunable optic filter with enhanced sidelobe suppression," *Electron. Lett.*, vol. 25, no. 6, pp. 398–399, 1989.
[22] F. W. Windels, V. I. Pustovoit, and O. Leroy, "Collinear acousto-optic diffraction using two nearby sound frequencies," *Ultrasonics*, vol. 38, pp. 586–589, 2000.
[23] K. B. Yushkov and V. Y. Molchanov, "MTF formalism for measurement of spectral resolution of acousto-optical devices with synthesized transmission function," *Opt. Lett.*, vol. 38, no. 18, pp. 3578–3780, 2013.
[24] S. N. Mantsevich and V. I. Balakshy, "Experimental examination of frequency locking effect in acousto-optic system," *Appl. Phys. B*, vol. 124, no. 54, pp. 1–17, 2018.
[25] S. N. Mantsevich and V. I. Balakshy, "Examination of optoelectronic feedback effect on collinear acousto-optic filtration," *J. Opt. Soc. Amer. B*, vol. 35, no. 5, pp. 1030–1039, 2018.
[26] V. I. Balakshy, Y. I. Kuznetsov, and S. N. Mantsevich, "Effect of optoelectronic feedback on the characteristics of acousto-optical collinear filtering," *Quantum Electron.*, vol. 46, no. 2, pp. 181–184, 2016.
[27] S. N. Mantsevich, V. I. Balakshy, and Y. I. Kuznetsov, "Acousto-optic collinear filter with optoelectronic feedback," *Appl. Phys. B*, vol. 123, no. 101, pp. 1–8, 2017.
[28] V. I. Balakshy, Y. I. Kuznetsov, S. N. Mantsevich, and N. V. Polikarpova, "Dynamic processes in an acousto-optic laser beam intensity stabilization system," *Opt. Laser Technol.*, vol. 62, pp. 89–94, 2014.
[29] V. I. Balakshy and I. A. Nagaeva, "Optoelectronic generator based on acousto-optical interaction," *Quantum Electron.*, vol. 26, no. 3, pp. 254–257, 1996.
[30] M. R. Chatterjee and M. Al-Saedi, "Examination of chaotic signal encryption and recovery for secure communication using hybrid acousto-optic feedback," *Opt. Eng.*, vol. 50, no. 5, 2011, Art. no. 055002.
[31] V. I. Balakshy, A. V. Kazaryan, and V. Y. Molchanov, "Deflectors with a feedback: New possibilities for image processing," *Proc. SPIE*, vol. 2051, pp. 672–677, 1993.
[32] T.-C. Poon and S.K. Cheung, "Performance of a hybrid bistable device using an acoustooptic modulator," *Appl. Opt.*, vol. 28, no. 22, pp. 4787–4791, 1989.
[33] S. Mantsevich, V. Balakshy, and Y. Kuznetsov, "Acousto-optic spectrum analyzer - the new type of optoelectronic device," in *Proc. 5th Int. Conf. Photon. Opt. Laser Technol.*, 2017, pp. 237–244.
[34] V. I. Balakshy and A. V. Kazaryan, "Laser beam direction stabilization by means of Bragg diffraction," *Opt. Eng.*, vol. 38, no. 7, pp. 1154–1159, 1999.
[35] J. Chrostrowski, R. Vallee, and C. Delisle, "Self-pulsing and chaos in acoustooptic bistability," *Can. J. Phys.*, vol. 61, no. 8, pp. 1143–1148, 1983.
[36] J. Chrostrowski, C. Delisle and R. Tremblay, "Oscillations in an acoustooptic bistable device," *Can. J. Phys.*, vol. 61, no. 2, pp. 188–191, 1983.
[37] M. R. Chatterjee and J.-J. Huang, "Demonstration of acousto-optic bistability and chaos by direct nonlinear circuit modeling," *Appl. Opt.*, vol. 31, no. 14, pp. 2506–2517, 1992.
[38] V. I. Balakshy, A. I. Bychkov, Y. I. Kuznetsov, and S. A. Shabunin, "Dynamic processes in acoustooptic system with amplitude feedback," *J. Commun. Technol. Electron.*, vol. 50, pp. 1169–1176, 2005.
[39] V. I. Balakshii, A. V. Kazar'yan, and A. A. Lee, "Multistability in an acousto-optical system with a frequency feedback," *Quantum Electron.*, vol. 25, no. 10, pp. 940–944, 1995.
[40] V. I. Balakshy and S. N. Mantsevich, "Influence of light polarization on characteristics of a collinear acoustooptic diffraction," *Opt. Spectrosc.*, vol. 106, no. 3, pp. 441–445, 2009.
[41] V. I. Balakshy and S. N. Mantsevich, "Polarization effects at collinear acousto-optic interaction," *Opt. Laser Technol.*, vol. 44, no. 4, pp. 893–898, 2012.
[42] S. E. Harris and R. W. Wallace, "Acoustooptic tunable filter," *J. Opt. Soc. Amer.*, vol. 59, no. 6, pp. 744–747, 1969.
[43] S. E. Harris, S. T. K. Nieh, and R. S. Feigelson, "CaMoO4 electronically tunable optical filter," *Appl. Phys. Lett.*, vol. 17, pp. 223–225, 1970.